Wang and Page-McCaw, http://www.jcb.org/cgi/content/full/jcb.201403084/DC1

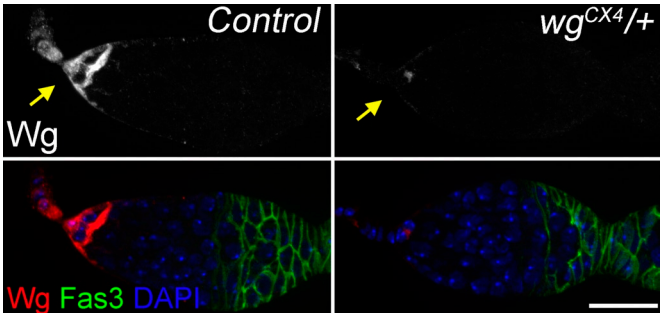

Figure S1. **Extracellular anti-Wg staining is specific.** Note the difference between wild type (w^{1118}) and *wg* heterozygote (w^{1118}; wg^{CX4}/CyO). Arrows denote Wg staining near cap cells. Bar, 20 µm.

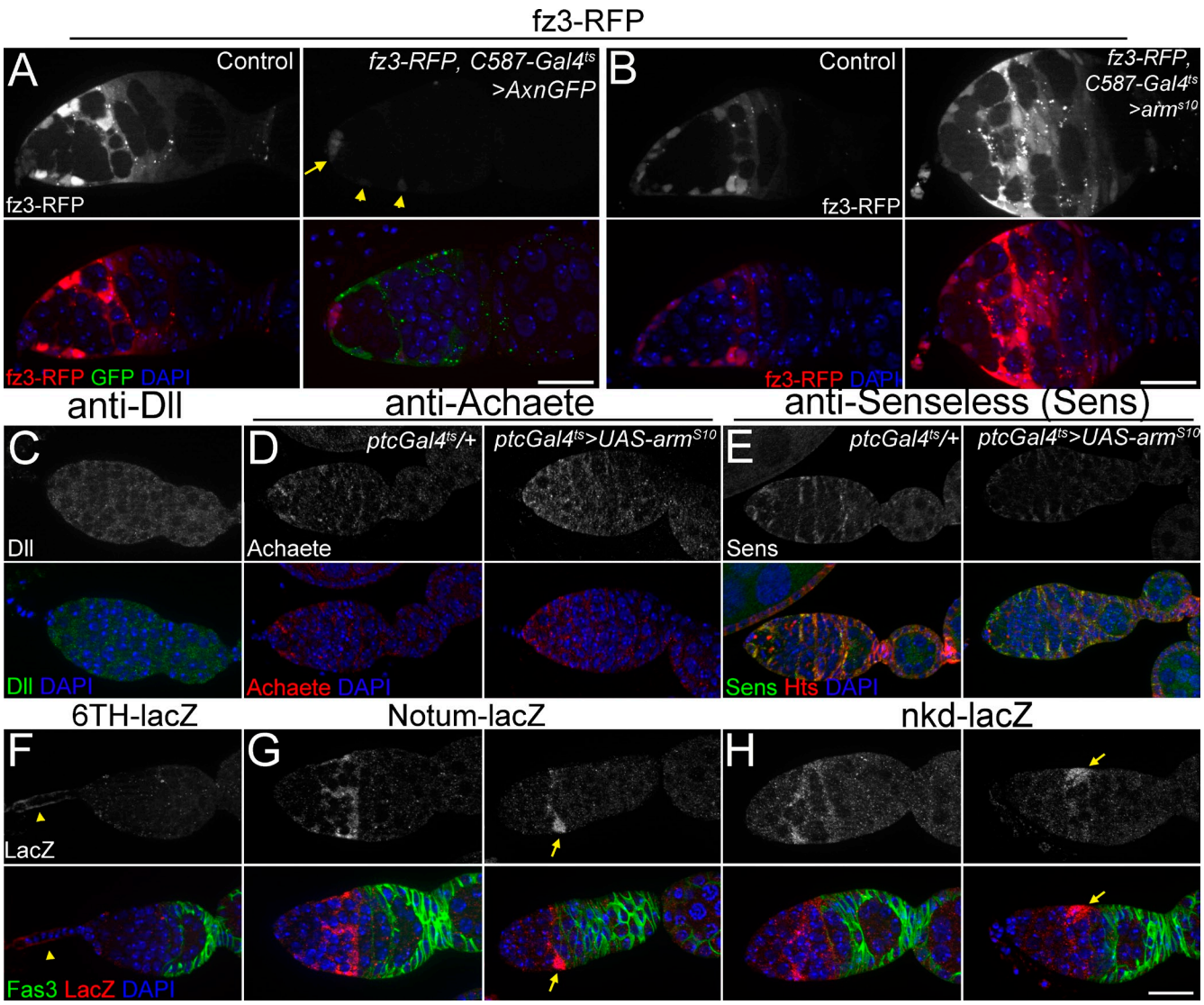

Figure S2. **Assessment of Wg activity-reporter candidates in the germaria.** (A and B) *fz3-RFP* responds to gain and loss of Wg signaling activity. *fz3-RFP* levels were reduced by the escort cell expression of GFP-tagged *Axn* (*w C587 Gal4/w; fz3-RFP/UAS-Axn-GFP*), a negative regulator of the Wg pathway. Residual activity was observed in cap cells (arrows) and two escort cells (A, arrowheads). In contrast, *fz3-RFP* levels were elevated when Wg signaling activity was increased by escort cell overexpression of arm^{S10}, a constitutively active form of *arm* (B; *w C587 Gal4/*y^{1} w^{1118} *UAS-*Arm^{S10}*; fz3-RFP/+*). Control genotype: *w C587 Gal4/*w^{1118}*; fz3-RFP/+*. (C) Anti-Distalless (Dll; 1:200, a gift from I. Duncan, Washington University, St Louis, MO), a long-range Wg signaling reporter in the wing disc (Neumann and Cohen, 1997; Zecca et al., 1996), did not show specific staining pattern in wild-type germarium (w^{1118}). (D and E) Anti-Achaete (D; 1:5; DSHB; Couso et al., 1994) or anti-Senseless (E; Sens, 1:1,000; a gift from H. Bellen, Baylor College of Medicine, Houston, TX; Nolo et al., 2000), two short-range Wg reporters in the wing disc, exhibited patterns that did not respond to overexpression of arm^{S10} (y^{1} w^{1118} *UAS-*Arm^{S10}*/w; ptcGal4/+; tubGal80*^{ts}*/+*), which suggests that the staining observed was probably nonspecific. Control genotype: *w; ptcGal4/+; tubGal80*^{ts}*/+*. (F) *SIXTH-lacZ* expresses *lacZ* downstream of six copies of TCF-helper sites and is a Wg activity reporter in embryos and eye discs (Chang et al., 2008b). In the germarium, *SIXTH-lacZ* signal was only found in terminal filament cells (arrowheads). (G and H) *Notum-lacZ* (Liu et al., 2008) and *nkd-lacZ* (Chang et al., 2008a), two reporters expressing *lacZ* downstream of the regulatory sequences of Wg feedback antagonists *Notum* and *naked cuticle* (*nkd*), respectively, showed variable patterns in escort cells and FSCs (arrows). LacZ reporters in F–H are gifts of K. Cadigan (University of Michigan, Ann Arbor, MI). C–H have the same magnification. Bars, 20 µm.

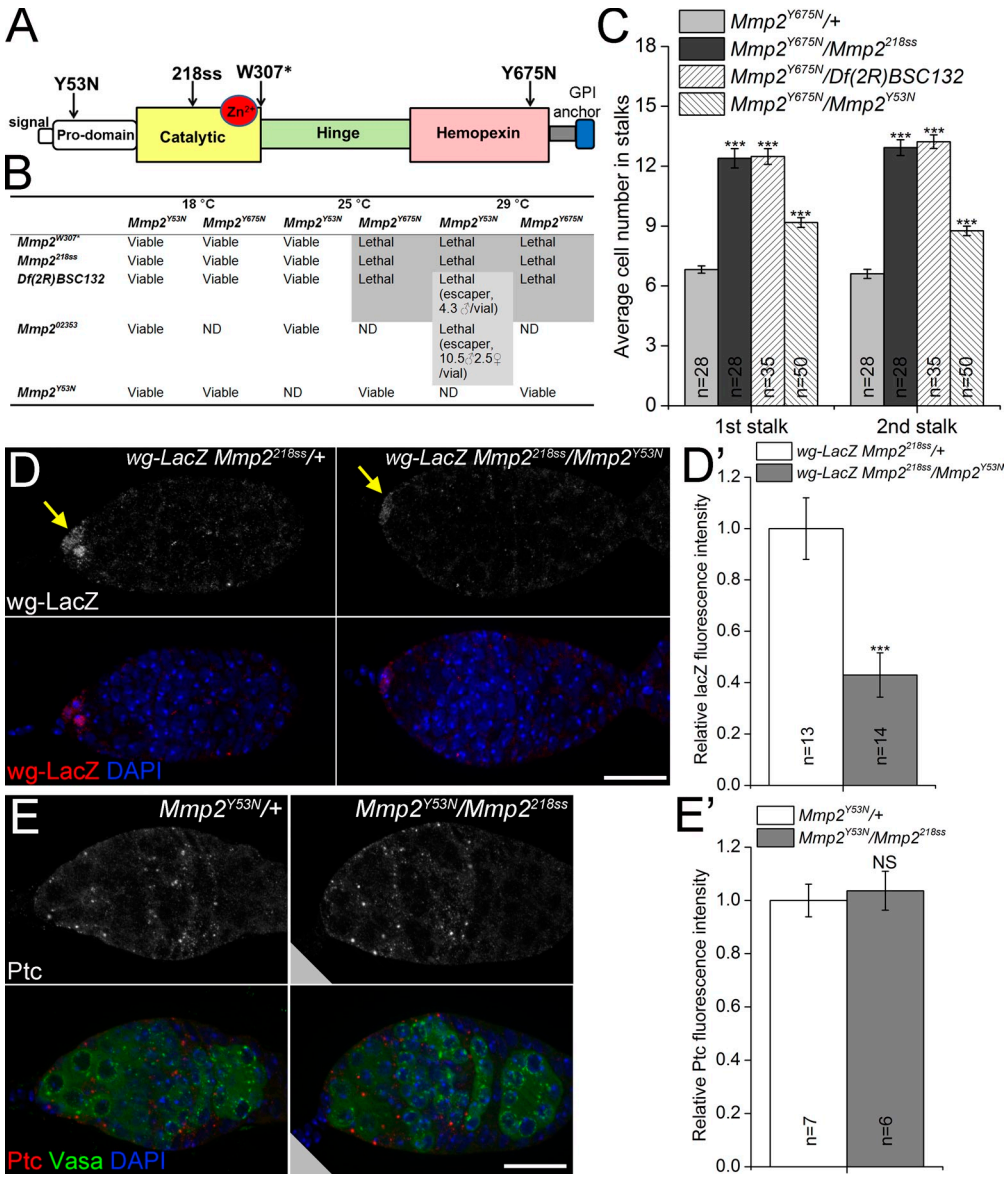

Figure S3. ***Mmp2* alleles and additional phenotypic description.** (A) Domain structure and EMS alleles of *Mmp2*. The asterisk represents the stop codon. 218ss allele contains a 3′ splice site mutation (AG at the 3′ splice site before exon 5 is mutated into AA; Page-McCaw et al., 2003). The Zn^{2+} binding region (HELGH) is at aa 257–261. Mmp2 contains a predicted GPI anchor site at S734. (B) Pupal lethality of *Mmp2* tran-heterozygotes raised at different temperatures. *Df(2R)BSC*132 is a large deficiency that completely disrupts the *Mmp2* gene region (Flybase). $Mmp2^{02353}$ is a P-element insertion in intron 3 of *Mmp2* (Page-McCaw et al., 2003). (C) Quantification of stalk cell numbers in $Mmp2^{Y675N}$ ts mutants 7–9 d after switching to 29°C. Significance is relative to $Mmp2^{Y675N}/+$ controls. All genotypes are in w^{1118} background. (D and D′) *Mmp2* mutants (w^{1118}; *wg-lacZ* $Mmp2^{218ss}/Mmp2^{Y53N}$) exhibited reduced levels of *wg-lacZ* transcriptional reporter. Control, w^{1118}; *wg-lacZ* $Mmp2^{218ss}/+$. Arrows, cap cells. (E and E′) The hedgehog pathway appeared unaffected in *Mmp2* mutants, as comparable levels of Ptc staining (1:4; DSHB) were observed in *Mmp2* mutants (w^{1118}; $Mmp2^{218ss}/Mmp2^{Y53N}$) and controls (w^{1118}; $Mmp2^{Y53N}/+$). Ptc staining appeared as speckles mainly in region 1 and region 2a, and the mean intensity was measured over the area of the germarium using ImageJ. ***, $P < 0.001$; NS, not significant (Student's *t* test). Error bars represent SEM. *n* indicates the number of germaria counted or imaged for quantification. Bars, 20 µm.

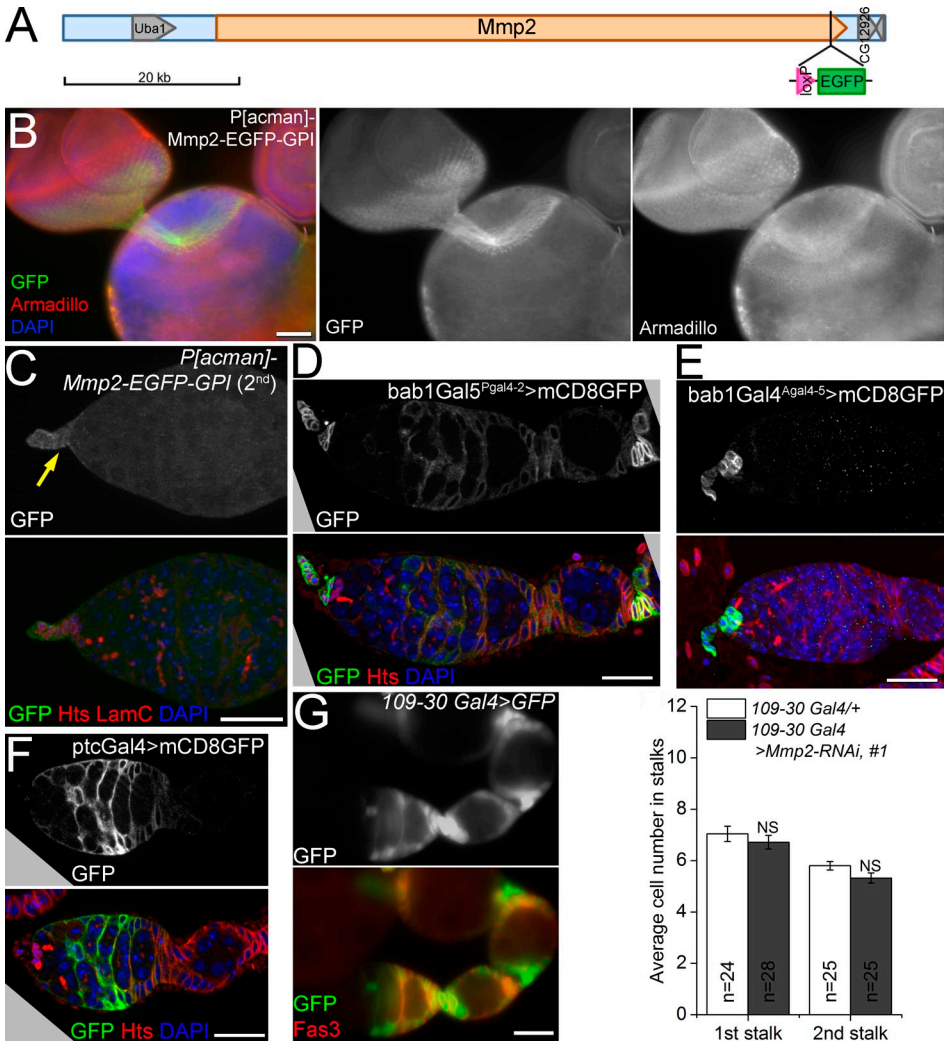

Figure S4. **Mmp2-EGFP-GPI structure and expression, GAL4 domains, and *Mmp2* knockdown in follicle cells.** (A) Diagram of the genomic BAC construct expressing EGFP-tagged Mmp2 under endogenous regulatory sequences. The BAC spans the whole *Mmp2* gene region (2R: 9,683,858–9,611,139, Berkeley Drosophila Genome Project *D. melanogaster* Release_6) and extends 17,480 bp in the 5′ direction and 3,575 bp in the 3′ direction. A sequence comprising a LoxP site and EGFP was inserted in-frame before the predicted GPI attachment site of Mmp2. (B) Expression of *P[acman]-Mmp2-EGFP-GPI* in larval optic lobe and eye disc (*y w; P{ P[acman]-Mmp2-EGFP-GPI}VK33*). GFP signal was observed in lamina in the optic lobe as well as in photoreceptors behind the morphogenetic furrow. (C) Expression of *P[acman]-Mmp2-EGFP-GPI* inserted on the second chromosome (*y w; P{P[acman]-Mmp2-EGFP-GPI}attP40*) in apical cells (arrow). (D) *bab1Gal4*$^{Pgal4\text{-}2}$ drives gene expression in apical cells and stalk cells, and weakly in escort cells and follicle cells, shown with UAS-mCD8GFP, a cell surface GFP (*w; UAS-mCD8GFP/+; bab1Gal4*$^{Pgal4\text{-}2}$*/+*). (E) *bab1Gal4*$^{Agal4\text{-}5}$ drives expression specifically in apical cells (*w; UAS-mCD8GFP/+; bab1Gal4*$^{Agal4\text{-}5}$*/+*). (F) *ptcGal4* drives expression in escort cells and FSCs, and weakly in follicle precursor cells (*w; UAS-mCD8GFP/ptcGal4*). (G) *Mmp2* was not required in follicle cells. *Mmp2* RNAi was driven by follicle cell driver *109-30 Gal4* (*w; UAS-GFP/109-30 Gal4*; expression pattern shown in G). NS, not significant, Student's *t* test. Error bars represent SEM. *n* indicates the number of germaria counted. Bars: (B) 50 µm; (all other panels) 20 µm.

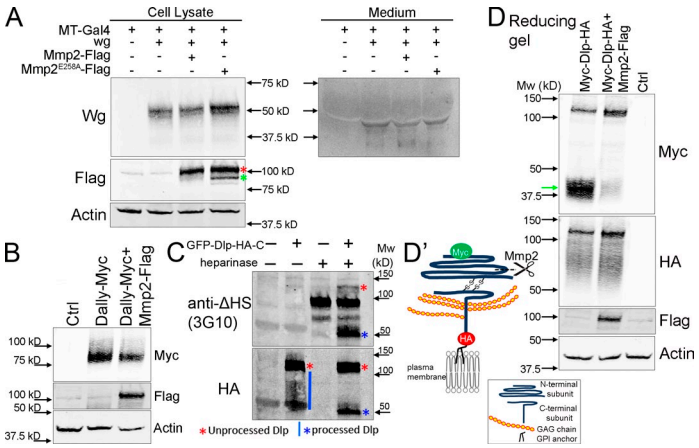

Figure S5. **Supplementary biochemical analysis.** (A) Mmp2 did not cleave Wg. S2 cells were transiently transfected with constructs expressing Wg or Mmp2 under a copper-inducible promoter. Wg protein was analyzed (anti-Wg, 4D4; DSHB) in cell lysates or conditioned medium (serum-containing, unconcentrated). Mmp2 ran as doublets (red and green asterisks) in lysates. (B–D) Western blots were performed on transiently transfected S2R+ cell lysates. (B) Mmp2 did not cleave Dally. Mmp2 coexpression did not change the size or amount of Dally tagged at the N terminus with Myc (Dejima et al., 2011; mouse anti–c-Myc, R950-25; Invitrogen). (C) Heparan sulfate chains were observed mainly on processed forms of Dlp. Without heparinase treatment (lane 2), Dlp was recognized by its C-terminal HA tag (red asterisks on the bottom gel, unprocessed Dlp; blue line, processed C-terminal Dlp containing GAG modifications running as a smear). Heparinase treatment (lane 4) collapsed the GAG-containing smear to a band (blue asterisk, bottom gel). Digestion of heparan sulfate GAGs with heparinase creates a neo-epitope recognized by the anti-ΔHS antibody (top gel). Note that processed Dlp (blue asterisk, top gel) had more abundant GAG modifications (anti-ΔHS, 3G10; US Biological) than the unprocessed form (red asterisk, top gel). (D and D') The cleavage of Dlp by Mmp2 was confirmed using a Dlp construct where the GFP tag was replaced by the Myc tag. The plasmid was constructed by replacing GFP in *pUAST-GFP-Dlp-HA-C* (Kreuger et al., 2004) with a 3× Myc sequence flanked by SphI sites. The N-terminal subunit of Dlp recognized by anti-Myc (green arrow, D) was absent when Flag-tagged Mmp2 was coexpressed. Actin, loading control.

References

Chang, J.L., M.V. Chang, S. Barolo, and K.M. Cadigan. 2008a. Regulation of the feedback antagonist naked cuticle by Wingless signaling. *Dev. Biol.* 321:446–454. http://dx.doi.org/10.1016/j.ydbio.2008.05.551

Chang, M.V., J.L. Chang, A. Gangopadhyay, A. Shearer, and K.M. Cadigan. 2008b. Activation of wingless targets requires bipartite recognition of DNA by TCF. *Curr. Biol.* 18:1877–1881. http://dx.doi.org/10.1016/j.cub.2008.10.047

Couso, J.P., S.A. Bishop, and A. Martinez Arias. 1994. The wingless signalling pathway and the patterning of the wing margin in Drosophila. *Development*. 120:621–636.

Dejima, K., M.I. Kanai, T. Akiyama, D.C. Levings, and H. Nakato. 2011. Novel contact-dependent bone morphogenetic protein (BMP) signaling mediated by heparan sulfate proteoglycans. *J. Biol. Chem.* 286:17103–17111. http://dx.doi.org/10.1074/jbc.M110.208082

Kreuger, J., L. Perez, A.J. Giraldez, and S.M. Cohen. 2004. Opposing activities of Dally-like glypican at high and low levels of Wingless morphogen activity. *Dev. Cell*. 7:503–512. http://dx.doi.org/10.1016/j.devcel.2004.08.005

Liu, Y.I., M.V. Chang, H.E. Li, S. Barolo, J.L. Chang, T.A. Blauwkamp, and K.M. Cadigan. 2008. The chromatin remodelers ISWI and ACF1 directly repress Wingless transcriptional targets. *Dev. Biol.* 323:41–52. http://dx.doi.org/10.1016/j.ydbio.2008.08.011

Neumann, C.J., and S.M. Cohen. 1997. Long-range action of Wingless organizes the dorsal-ventral axis of the Drosophila wing. *Development*. 124:871–880.

Nolo, R., L.A. Abbott, and H.J. Bellen. 2000. Senseless, a Zn finger transcription factor, is necessary and sufficient for sensory organ development in Drosophila. *Cell*. 102:349–362. http://dx.doi.org/10.1016/S0092-8674(00)00040-4

Page-McCaw, A., J. Serano, J.M. Santé, and G.M. Rubin. 2003. Drosophila matrix metalloproteinases are required for tissue remodeling, but not embryonic development. *Dev. Cell*. 4:95–106. http://dx.doi.org/10.1016/S1534-5807(02)00400-8

Zecca, M., K. Basler, and G. Struhl. 1996. Direct and long-range action of a wingless morphogen gradient. *Cell*. 87:833–844. http://dx.doi.org/10.1016/S0092-8674(00)81991-1